



Article

# A Leucine-Rich Repeat Receptor-like Kinase TaBIR1 Contributes to Wheat Resistance against *Puccinia striiformis* f. sp. *tritici*

Yingchao Sun, Xiaojie Wang, Feiyang Liu, Haoyu Guo, Jianfeng Wang, Zetong Wei, Zhensheng Kang \*  and Chunlei Tang \*

State Key Laboratory of Crop Stress Biology for Arid Areas and College of Plant Protection, Northwest A&F University, Xianyang 712100, China; sunyc316@nwfau.edu.cn (Y.S.); wangxiaojie@nwsuaf.edu.cn (X.W.); liufeyang@nwafu.edu.cn (F.L.); ghy2611625@nwafu.edu.cn (H.G.); ipp@nwsuaf.edu.cn (J.W.); wzt132@nwafu.edu.cn (Z.W.)

\* Correspondence: kangzs@nwsuaf.edu.cn (Z.K.); tangchunlei@nwafu.edu.cn (C.T.)

**Abstract:** Plant cell surface-localized receptor-like kinases (RLKs) recognize invading pathogens and transduce the immune signals inside host cells, subsequently triggering immune responses to fight off pathogen invasion. Nonetheless, our understanding of the role of RLKs in wheat resistance to the biotrophic fungus *Puccinia striiformis* f. sp. *tritici* (*Pst*) remains limited. During the differentially expressed genes in *Pst* infected wheat leaves, a Leucine-repeat receptor-like kinase (LRR-RLK) gene *TaBIR1* was significantly upregulated in the incompatible wheat-*Pst* interaction. qRT-PCR verified that *TaBIR1* is induced at the early infection stage of *Pst*. The transient expression of TaBIR1-GFP protein in *N. benthamiana* cells and wheat mesophyll protoplasts revealed its plasma membrane location. The knockdown of *TaBIR1* expression by VIGS (virus induced gene silencing) declined wheat resistance to stripe rust, resulting in reduced reactive oxygen species (ROS) production, callose deposition, and transcripts of pathogenesis-related genes *TaPR1* and *TaPR2*, along with increased *Pst* infection area. Ectopic overexpression of *TaBIR1* in *N. benthamiana* triggered constitutive immune responses with significant cell death, callose accumulation, and ROS production. Moreover, *TaBIR1* triggered immunity is dependent on *NbBAK1*, the silencing of which significantly attenuated the defense response triggered by *TaBIR1*. *TaBIR1* interacted with the *NbBAK1* homologues in wheat, co-receptor TaSERK2 and TaSERK5, the transient expression of which could restore the impaired defense due to *NbBAK1* silencing. Taken together, *TaBIR1* is a cell surface RLK that contributes to wheat stripe rust resistance, probably as a positive regulator of plant immunity in a *BAK1*-dependent manner.

**Keywords:** cell surface receptor-like kinases (RLKs); stripe rust; immune responses; co-receptor



**Citation:** Sun, Y.; Wang, X.; Liu, F.; Guo, H.; Wang, J.; Wei, Z.; Kang, Z.; Tang, C. A Leucine-Rich Repeat Receptor-like Kinase TaBIR1 Contributes to Wheat Resistance against *Puccinia striiformis* f. sp. *tritici*. *Int. J. Mol. Sci.* **2023**, *24*, 6438. <https://doi.org/10.3390/ijms24076438>

Academic Editor: Ivan Kreft

Received: 12 March 2023

Revised: 19 March 2023

Accepted: 24 March 2023

Published: 29 March 2023



**Copyright:** © 2023 by the authors. Licensee MDPI, Basel, Switzerland. This article is an open access article distributed under the terms and conditions of the Creative Commons Attribution (CC BY) license (<https://creativecommons.org/licenses/by/4.0/>).

## 1. Introduction

Plants deploy cell surface-localized pattern recognition receptors (PRRs) for perceiving conserved molecules, such as pathogen/microbe-associated molecular patterns (PAMPs/MAMPs) or damage-associated molecular patterns (DAMPs) to trigger PAMP-triggered immunity (PTI) [1,2]. As the first layer of plant immunity, PTI is critical for plants to survive under the threat of numerous pathogenic microbes. The second layer is effector-triggered immunity (ETI), which is specifically dependent on the direct or indirect recognition of avirulence (*Avr*) effectors by cytoplasmic immune receptors, mainly the nucleotide-binding site (NBS) and leucine-rich repeat (LRR) class [3,4]. PTI defenses include the rapid ion fluxes, burst of reactive oxygen species (ROS), deposition of callose, activation of mitogen-activated protein kinases (MAPKs), and the expression of immune-related genes, while ETI events generally leads to robust hypersensitive response (HR), characterized by rapid and local cell death at the infection sites [4,5]. Recent studies demonstrated

that some PRRs in PTI are also required for ETI, and the two immune signal pathways are potentiated and interconnected [6,7].

An increasing number of plant cell-surface receptors have been identified, all of which are reported to encode receptor-like kinases (RLKs) or receptor-like proteins (RLPs) [8]. RLKs contain a ligand-binding ectodomain, a transmembrane domain and an intracellular kinase domain, while RLPs lack the intracellular kinase domain. The ectodomain of them are quite divergent, thus allowing RLKs respond to different signals. Leucine-rich repeats (LRR)-containing receptor-like kinases (LRR-RLKs) represent the largest group of RLKs, with at least 223 members in Arabidopsis [9]. The two typical LRR-RLK in Arabidopsis FLAGELLIN SENSING 2 (FLS2) and EFR (Elongation Factor-Tu Receptor) recognize bacteria flg22 and the short, conserved N-terminal of the most abundant bacterial protein elongation factor-Tu though their extracellular LRRs, respectively [10–12]. The recognition of flg22 by FLS2 activates the intracellular kinase BIK1, which in turn causes phosphorylation of the NADPH oxidase RBOHD on plasma membrane and results in production of large amounts of ROS. Meanwhile, the intracellular PBL kinase are phosphorylated followed by activation of MEKK1-MKK1/2-MPK4 and MAPKKK3/5-MKK4/5-MPK3/6 signaling pathways [13–16]. The recognition of EFR and bacterial elf18 can activate the same downstream immune signal pathway as FLS2-flg22 [12]. Rice resistance gene XA21, encoding an LRR-RLK, recognizes the highly conserved Ax21 of *Xanthomonas oryzae* and confers broad spectrum resistance to the Gram-negative bacterium *Xanthomonas oryzae* pv. *oryzae* [17,18]. Although LRR-RLPs lack cytoplasmic domains, their function is similar to that of LRR-RLKs. The heterodimer formed by receptor protein CEBiP and CERK1 activates the downstream OsRLCK185 and MAPK cascades to mediate chitin signal transduction [19–23]. Generally, to date numerous LRR-RLKs are identified as crucial components in regulating plant immune responses.

RLK/RLP is usually associated with co-receptors to form extracellular immune receptor complex on the cell surface to transmit extracellular immune signal [1,8]. To date, almost all the identified PRRs rely on somatic embryogenesis receptor kinases (SERKs) or SOBIR1 [24,25]. SERKs directly complex with PAMP/MAMPs receptors upon ligand perception. For example, the Arabidopsis BAK1 (BRI1-ASSOCIATED KINASE 1), also known as SERK3, interacts with FLS2 or EFR upon flg22 or elf18 ligand perception [11,26]. BIR1 and BIR2 (BAK1-interacting receptor-like kinase), interacts with BAK1 and negatively regulates PRR complex in immunity [27,28]. In the absence of stimuli, BIR2 inhibits BAK1 interaction with FLS2. Upon perception of flg22, BIR2 dissociates from BAK1, thus allowing BAK1-FLS2 formation to trigger immune responses [27,29]. Arabidopsis SERK4 functions redundantly with SERK3 in regulating cell death containment and immunity [30]. Rice BAK1 orthologous OsSERK2 forms a constitutive complex with XA21 that confers resistance to *Xanthomonas oryzae* pv. *oryzae*. OsSERK2 is also required for XA3-mediated immunity as well as rice FLS2 signaling [31]. In tomato, SISRK3 acts as positive regulator and is required for *Ve1*-mediated resistance to fungal *Verticillium* [32]. Therefore, SERK receptors interact with a broad array of receptors to modulate the immune signaling which may suggest they remain at the center stage for studying the roles of RLK.

The existing evidence shows that the immune pathway mediated by extracellular receptors is conservative among plant species. However, in contrast to the well-studied PRRs in model plants Arabidopsis, the characterization of key extracellular receptors in the major food crop wheat is very limited, especially during wheat–*Puccinia striiformis* f. sp. *tritici* (*Pst*) interaction. *Pst* is an obligate biotrophic fungus, causing devastating stripe rust disease on wheat worldwide. There is a lack of systematic and in-depth research on the role and regulation mechanism of extracellular receptors on wheat resistance to stripe rust. As a widely used experimental plant, *Nicotiana benthamiana* is susceptible to a wide variety of pathogens and provides facile methods such as virus-induced gene silencing or transient protein expression, making it a cornerstone for studying innate immunity and defense signaling in host-pathogen research [33].

In the present study, we functionally characterized a cell-surface located wheat LRR-RLK gene *TaBIR1*, which is highly induced upon avirulent *Pst* infection. Knockdown of *TaBIR1* significantly impaired wheat resistance to stripe rust and transient expression of *TaBIR1* triggered constitutive defense response in *N. benthamiana* requiring *NbBAK1*. Moreover, we revealed that *TaBIR1* interacts with *TaSERK2* and *TaSERK5*, which could restore the deficiency of *NbBAK1* in triggering plant immunity. The present investigation aimed to identify a wheat LRR-RLK *TaBIR1* that positively regulates wheat resistance to stripe rust, which probably associates with *TaSERK2* and *TaSERK5* to confer immunity.

## 2. Results

### 2.1. *TaBIR1* Encodes a Conserved LRR-X Family Serine/Threonine Kinase

Among the differentially expressed genes in *Pst* infected wheat leaves analyzed by cDNA-AFLP [34], a transcript derived fragment (PST\_576-6) is significantly upregulated with 5-fold in *Pst*-wheat interaction. Full-length cDNA cloning revealed an open reading frame (ORF) of 1,818 bp encoding a receptor-like kinase (RLK), which contains a signal peptide, extracellular LRRs (leucine rich repeats), a transmembrane region and a cytoplasmic kinase domain (Figure S1A). Multiple alignments showed that this RLK displays conserved kinase subdomains across its homologues in other monocot and dicot plants, and shares 65.9% similarity to *BIR1* (AT5G48380) in Arabidopsis (Figure S1B) that is classified into LRR-X subgroup. We thus named it *TaBIR1* (for *Triticum aestivum* BAK-Interacting Receptor-like kinase1). There are three homologues of *TaBIR1* located at chromosome 1A, 1B and 1D in wheat genome. The coding sequence of the three homologues of *TaBIR1* are 97.8% identical at the nucleotide level and have variations in 43 amino acids (Figure S2A). Phylogenetic analyses revealed that *TaBIR1* is mostly close to BAJ86446.1 in *Hordeum vulgare* (Figure S2B).

qRT-PCR analyses showed that avirulent *Pst* CYR23 infection upregulated *TaBIR1* at the early infection stage such as 6 h post infection (hpi) and reaches the peak at 24 hpi, about 15-fold higher than that at 0 hpi (Figure 1). By contrast, the expression of *TaBIR1* were not obviously induced by the virulent *Pst* CYR31 infection (Figure 1). These results suggest that the expression of *TaBIR1* is induced in early avirulent *Pst* infection stages.

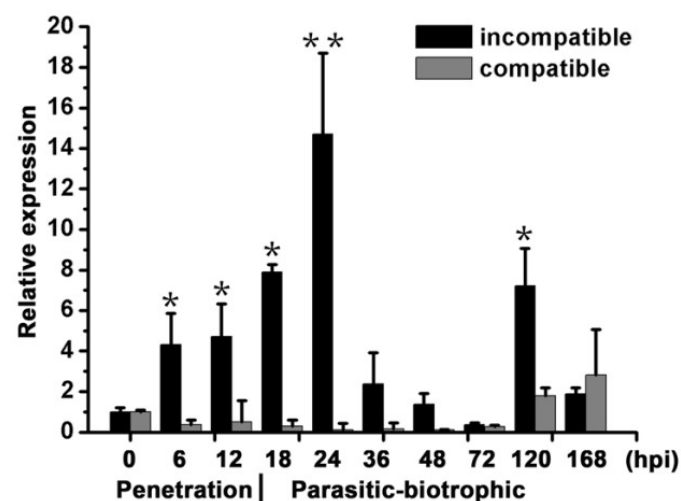


**Figure 1.** Expression profile of *TaBIR1* during wheat-*Pst* interaction. The second leaves of wheat cultivar Suwon11 were inoculated with fresh urediospores of avirulent *Pst* race CYR23 (incompatible interaction) or virulent *Pst* race CYR31 (compatible interaction) and sampled at different hours post-inoculation (hpi) for RNA extraction. Relative transcript levels of *TaBIR1* were calculated by the comparative threshold ( $2^{-\Delta\Delta CT}$ ) method and normalized to the transcript level of *TaEF*. Values represent the means  $\pm$  standard errors of three independent biological replicates. Asterisks indicate significant differences (\*  $p < 0.05$ , \*\*  $p < 0.01$ ) comparing to *TaBIR1* expression level at 0 hpi using Student's *t*-tests.

## 2.2. *TabIR1* Localizes to the Plasma Membrane

*TabIR1* contains a predicted transmembrane domain, indicating its plasma membrane location. We examined its subcellular localization through transiently expressing green fluorescent protein (GFP) fused *TabIR1* by the cauliflower mosaic virus 35S promoter in *N. benthamiana*. The control cells expressing GFP alone showed a nuclear/cytoplasmic/plasma membrane distribution, while the fluorescence of *TabIR1*-GFP fusion protein was confined to the cell surface (Figure 2A). To rule out the interference of plant cell wall, we next performed plasmolysis treatment. Green fluorescence was clearly visualized on the separated plasma membrane in cells expressing *TabIR1*-GFP, suggesting the plasma membrane-localization of *TabIR1*-GFP (Figure 2A). Immunoblotting analyses detected the corresponding bands of GFP and *TabIR1*-GFP, indicating their successful expression (Figure 2B). To further confirm the plasma membrane localization of *TabIR1*, we expressed *TabIR1*-GFP in wheat mesophyll protoplasts. *TabIR1*-GFP signal was observed on the plasma membrane of wheat cells (Figure 2C). Taken together, these data proved that *TabIR1* is localized on the plasma membrane.

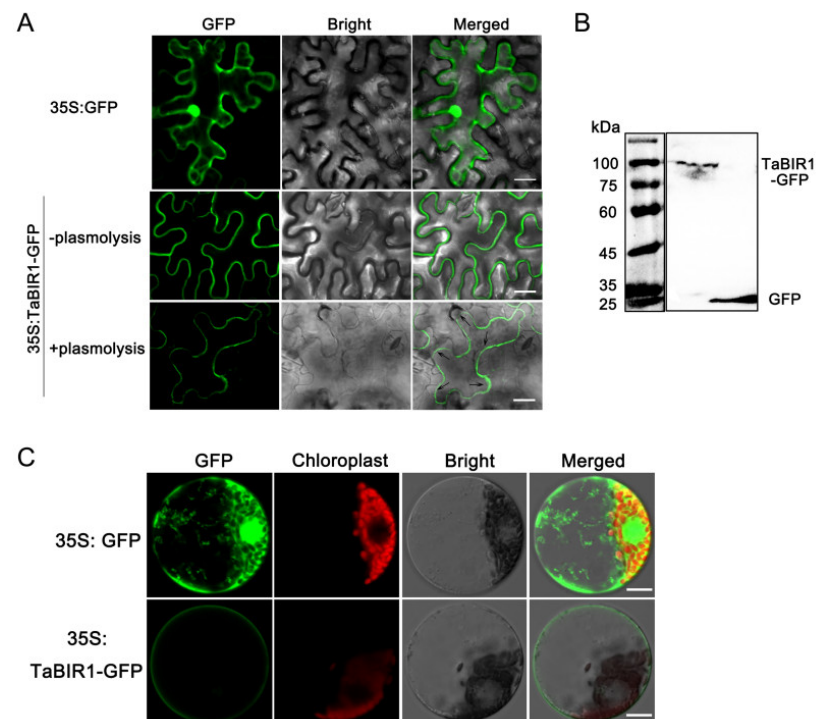


**Figure 2.** Subcellular localization of the *TabIR1*-GFP. (A) Agrobacterium-mediated transient expression of GFP and *TabIR1*-GFP driven by 35S promoter in *Nicotiana benthamiana* leaves. Fluorescence was observed under confocal microscopy at 48 h post infiltration. Arrows indicate the plasma membrane after plasmolysis treatment. Bars, 20  $\mu$ m. (B) Protein Western blot of *TabIR1*-GFP and GFP using anti-GFP polyclonal antibody. Protein ladder marker is shown at left. (C) Transient expression of GFP and *TabIR1*-GFP under 35S promoter in wheat mesophyll cell protoplasts using PEG-mediated transformation. Images were taken under confocal microscopy. Bars, 20  $\mu$ m.

## 2.3. Silencing of *TabIR1* Compromise Wheat Resistance against *Pst*

To investigate the function of *TabIR1* in wheat resistance to stripe rust, we transiently knocked down the expression of *TabIR1* in wheat using Barely Stripe Mosaic Virus (BSMV) mediated gene silencing (VIGS). Twelve days after BSMV inoculation on the second leaves, the fourth leaves of BSMV-infected plants appeared chlorotic mosaic symptoms, and wheat plants inoculated with BSMV:*TaPDS* showed obvious photobleaching, indicating the efficacy of virus-induced gene silencing (Figure 3A). At sixteen days post-inoculation of avirulent *Pst* race CYR23, the fourth leaves of control plants inoculated with BSMV:*GFP*

exhibited significant hypersensitive response (HR) without sporulation, while a few uredinospore pustules were formed on wheat leaves of *TaBIR1*-knockdown plants (Figure 3B). Silence efficiency analyses showed that *TaBIR1* was downregulated by 54.2%, 81.8% to 64.7% at 0, 24 and 48 hpi (Figure 3C). qPCR revealed that fungal biomass in *TaBIR1*-knockdown plants was increased by 55.1% than that in the control plants at 10 dpi (Figure 3D). Histological observation showed larger infection area of *Pst* in *TaBIR1* silenced leaves at 120 hpi compared to that in the control leaves (Figure 3E,F), suggesting the promoted *Pst* growth and development in *TaBIR1*-knockdown plants. These data demonstrated that silencing of *TaBIR1* compromised wheat resistance against *Pst*.

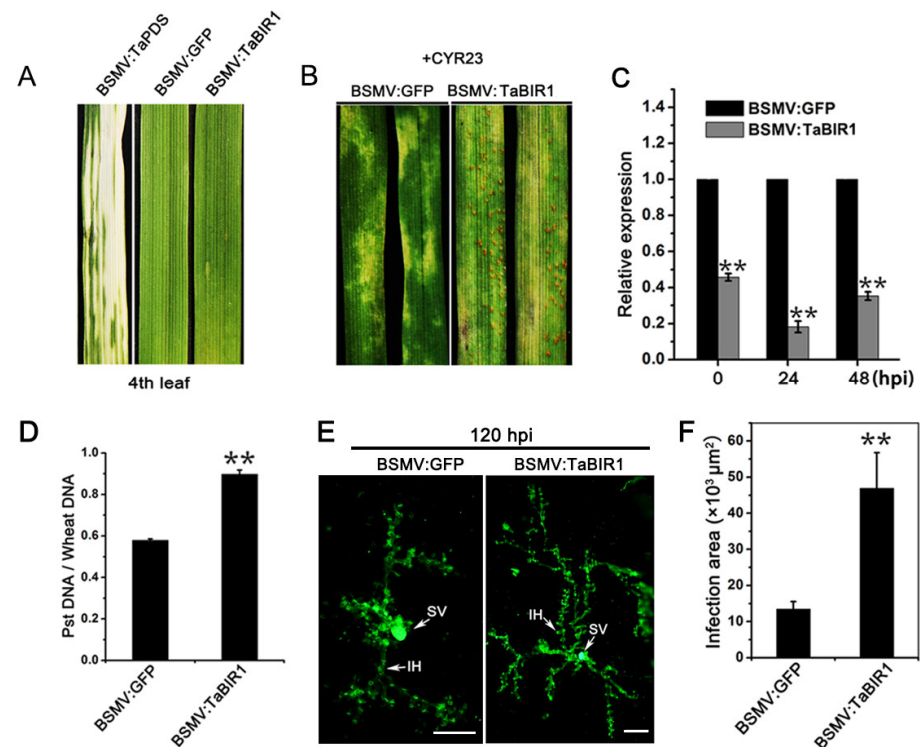


**Figure 3.** Transient silencing of *TaBIR1* via VIGS compromised wheat resistance to stripe rust. (A) Symptoms on the fourth leaves of wheat seedlings inoculated with BSMV:*TaPDS*, BSMV:*GFP* (negative control) and BSMV:*TaBIR1*. The second leaves of wheat cultivar Su11 were inoculated with recombinant BSMV and the virus phenotype were taken at 12 days post-inoculation (dpi). (B) Disease phenotypes of *TaBIR1*-silenced plants inoculated with *Pst* race CYR23 observed at 16 dpi. At 12 days post BSMV infection, the fourth leaves of wheat seedlings inoculated with BSMV:*GFP* and BSMV:*TaBIR1* were further challenged with avirulent *Pst* race CYR23. (C) Silencing efficiency of *TaBIR1* in *TaBIR1*-silenced plants at 0, 24 and 48 h post-inoculation (hpi) by qRT-PCR. (D) Relative *Pst* biomass in *TaBIR1*-silenced plants at 10 dpi. *PsEF* and *TaEF* were used as the internal reference genes. (E) Histological observation of *Pst* fungal development in *TaBIR1*-silenced plants at 120 hpi. SV, substomatal vesicle; IH, infection hyphae. Bars, 50  $\mu\text{m}$ . (F) *Pst* infection area per infection site in *TaBIR1*-silenced plants at 120 hpi. In (C,D,F), asterisks indicate significant differences compared with controls using Student's *t*-tests (\*\*  $p < 0.01$ ).

To further characterize the decreased wheat resistance, we examined the host immune responses in *TaBIR1* silenced plants. DAB staining showed decreased  $\text{H}_2\text{O}_2$  accumulation per infection site in *TaBIR1* silenced leaves than in control plants at 24 hpi (Figure 4A). Total ROS in *TaBIR1* silenced leaves was 57.6% less than that in control plants at 24 hpi (Figure 4B). In addition, the callose deposition was decreased by 69.4% in *TaBIR1* plants at 24 hpi (Figure 4C,D). The expression level of the defense related genes *TaPR1* and *TaPR2* were downregulated by 60.9% and 64.5%, respectively, in *TaBIR1* silenced plants

(Figure 4E,F). The results together suggested that silencing of *TaBIR1* led to defective immune responses, indicating the positive role of *TaBIR1* in wheat resistance to stripe rust.

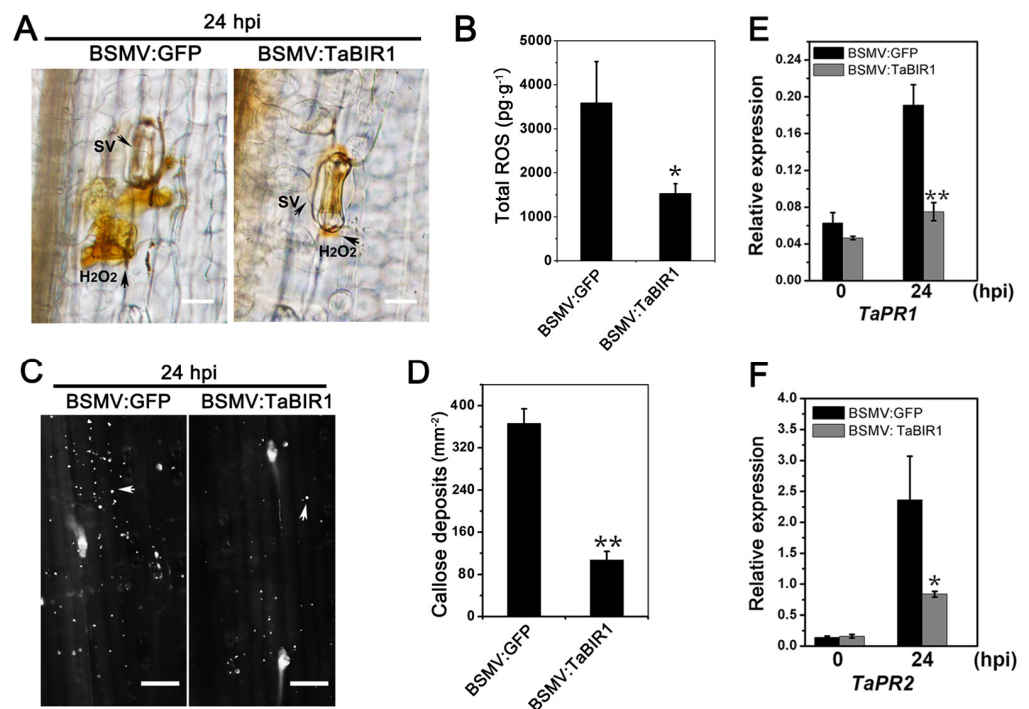


**Figure 4.** Impaired defense responses in *TaBIR1*-silenced plants. (A) Observation of DAB stained  $H_2O_2$  in *Pst* infected *TaBIR1*-silenced plants at 24 hpi. Bars, 20  $\mu m$ . (B) Determination of ROS production in *TaBIR1*-silenced plants. The fourth leaves of wheat seedlings inoculated with BSMV:GFP and BSMV:TaBIR1 were collected at 24 hpi for ROS content detection using HRP-labeled method. (C) Reduced callose deposition in *TaBIR1*-silenced plants. The fourth leaves of wheat seedlings inoculated with BSMV:GFP and BSMV:TaBIR1 were collected for aniline blue staining. White arrows shows the callose deposites. Bars, 50  $\mu m$ . (D) Quantification of the number of callose deposits per  $mm^2$ . Data are mean  $\pm$  standard errors ( $n = 30$ ) from three independent biological replicates. \*\*  $p < 0.01$  (E,F) Expression profile of pathogenesis related genes *TaPR1* and *TaPR2* in *TaBIR1*-silenced plants using qRT-PCR. Wheat *TaEF-1 $\alpha$*  was used as the internal reference gene. \*  $p < 0.05$ , \*\*  $p < 0.01$ . Three biological replicates were performed.

#### 2.4. Transient Over-Expression of *TaBIR1* in *N. benthamiana* Triggered Defense Responses

*TaBIR1* homologue in *Arabidopsis* is well known in basal immunity modulation, we therefore analyzed the basal roles of *TaBIR1* in plant defense. Aniline blue staining showed that heterologous expression of *TaBIR1* in *N. benthamiana* induce significantly more abundant callose deposition accumulation comparing to expressing GFP alone (Figure 5A,B). Additionally, dramatically increased ROS content were detected in *TaBIR1*-GFP expressed leaves at 36 and 48 h compared to that in leaves expressing GFP alone (Figure 5C), and significant ROS production was observed by DAB staining in *N. benthamiana* leaves expressing *TaBIR1*-GFP (Figure 5D). Along with that, trypan blue staining assay showed extensive cell death occurred at 48 h after expressing *TaBIR1*-GFP (Figure 5E), even though it could not trigger a visible cell death. In addition, *TaBIR1*-GFP expression upregulated the expression of *NbPR1* and *NbPR2* (Figure 5F). These findings strongly suggested that *TaBIR1* could induce constitutive immune responses and cell death in *N. benthamiana*.

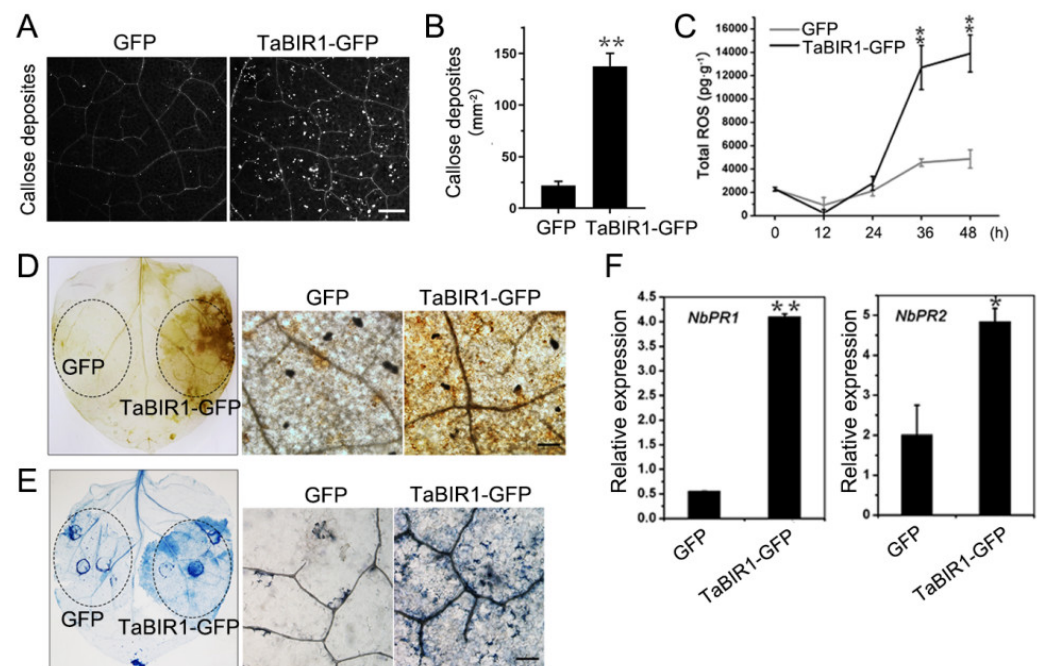


**Figure 5.** Transient expression of *TaBIR1* triggered immune responses in *Nicotiana benthamiana*. (A) Callose deposition stained by aniline blue in *N. benthamiana* leaves expressing GFP (the negative control) and TaBIR1-GFP. Bars, 200  $\mu$ m. (B) Quantification of callose deposits per mm<sup>2</sup>. Values represent the means  $\pm$  standard errors (n = 30). The experiment was repeated three times with similar results. \*\*  $p < 0.01$  using two tails unpaired Student's *t*-tests. (C) Determination of total ROS content in leaf tissue at different time points after infiltration. (D) DAB staining of H<sub>2</sub>O<sub>2</sub> production in *N. benthamiana* leaves expressing GFP and TaBIR1-GFP proteins. Scale bars, 100  $\mu$ m. (E) Trypan blue staining of cell death in leaves expressing GFP and TaBIR1-GFP at 48 h after infiltration. Scale bars, 100  $\mu$ m. (F) qRT-PCR analysis of *NbPR1* and *NbPR2* in *TaBIR1* expressing plant leaves. Values represent the means  $\pm$  standard errors of three independent biological samples. Asterisks indicate significant differences compared with GFP control using Student's *t*-tests. \*  $p < 0.05$ , \*\*  $p < 0.01$ .

### 2.5. *NbBAK1* Is Required for *TaBIR1* Mediated Cell Death and Immune Responses in *N. benthamiana*

Growing number of LRR-containing RLKs (and RLPs) are reported to engage in plant defense dependent on co-receptors, mainly *BAK1* or related *SERK* (Somatic embryogenesis receptor-like kinase), and *SOBIR1* [24,35,36]. To test whether *TaBIR1* mediated responses in *N. benthamiana* was dependent on *BAK1* or *SOBIR1*, we transiently silenced *NbBAK1* and *NbSOBIR1* using TRV-mediated gene silencing. qRT-PCR analyses revealed that *NbSOBIR1* and *NbBAK1* expression were reduced by 88.9% and 59.6%, respectively, comparing to that in control leaves inoculated with TRV2:GFP (Figure 6A,B). In *NbBAK1* silenced leaves, transient expression of *TaBIR1* resulted in significantly reduced callose deposition compared to that in the control leaves, while no obvious change in *NbSOBIR1* silenced leaves (Figure 6C,D). *TaBIR1* triggered ROS accumulation and cell death were also clearly attenuated by *NbBAK1* silencing (Figure 6E,F), so as the expression of *NbPR1* and *NbPR2* (Figure 6G,H). These results suggested that *NbBAK1* is required for *TaBIR1* mediated immune responses in *N. benthamiana*.

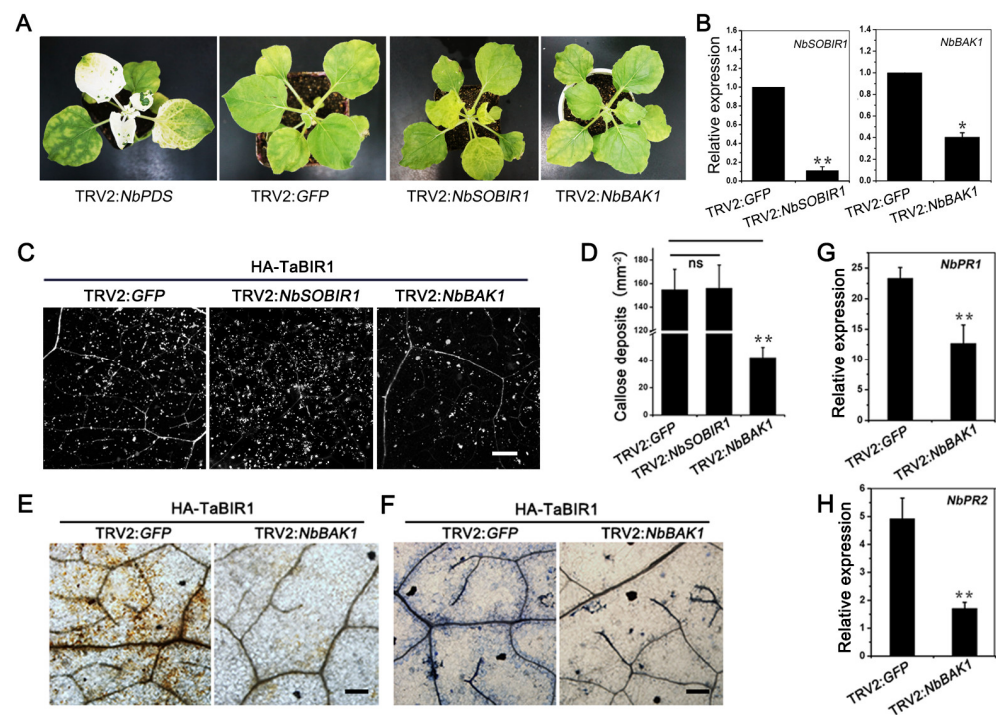


**Figure 6.** *NbBAK1* is required for *TaBIR1* triggered immunity. (A) Transient silencing of *NbSOBIR1* and *NbBAK1* in *N. benthamiana* mediated by tobacco rattle virus (TRV). Photobleaching was observed on plant leaves inoculated with TRV2:*PDS* two weeks later. GFP, negative control. (B) Silencing efficiency of *NbSOBIR1* and *NbBAK1* analyzed by qRT-PCR. Values represent the means  $\pm$  standard errors using Student's *t*-tests. (\*  $p < 0.05$ , \*\*  $p < 0.01$ ) (C,D) Transient silencing of *NbBAK1* reduced callose reposition triggered by *TaBIR1* in *N. benthamiana*. Plant leaves were inoculated with TRV2:*NbBAK1*, TRV2:*NbSOBIR1* and TRV2:*GFP*, on which two weeks later HA tagged *TaBIR1* was transiently expressed via agrobacterium mediated infiltration. Forty-eight hours post infiltration, the leaves were stained by aniline blue for callose deposition observation. The number of callose deposits per mm<sup>2</sup> was quantified. TRV2:*GFP* was used as the negative controls. Bars, 300  $\mu$ m. ns, no significance, \*\*  $p < 0.01$ . Data are means  $\pm$  standard errors from three biological replications. (E) Observation of DAB stained H<sub>2</sub>O<sub>2</sub> and (F) trypan blue stained cell death in *GFP* and *NbBAK1* silenced leaves expressing HA-*TaBIR1*. Bars, 100  $\mu$ m. (G,H) qRT-PCR analysis of *NbPR1* and *NbPR2* expression. Values represent the means  $\pm$  standard errors. \*\*  $p < 0.01$ , significant differences from three biological replicates using two-tails unpaired Student's *t*-tests.

### 2.6. *TaSERK2* and *TaSERK5* Interact with *TaBIR1* and Could Restore Impaired Defense Due to *NbBAK1* Silencing

There are multiple *SERK* genes and *SERK-like* genes in wheat. Previously five *SERK* homologous genes were cloned from the wheat genome sequences based on characteristic features of *SERKs* [37,38]. Here, we successfully obtained four of them in wheat variety Su11, named *TaSERK1*, *TaSERK2*, *TaSERK3*, *TaSERK5*. The four *TaSERKs* encode typical LRR-RLKs sharing similar protein domains (Figure S3). In *N. benthamiana* leaves co-expressing *TaBIR1*:cLUC with *TaSERK2*:nLUC or *TaSERK5*:nLUC, significant luciferase activity were detected, while no activity were observed in leaves co-expressing *TaBIR1*:cLUC and *TaSERK1*:nLUC, or *TaSERK3*:nLUC using split luciferase complementation (SLC) assay (Figure 7A). The results indicated that *TaBIR1* could interact with *TaSERK2* and *TaSERK5*, but not with *TaSERK1* and *TaSERK3* in *N. benthamiana*. To further verify the interaction, we performed co-immunoprecipitation (co-IP) assay in planta using intracellular domains of *TaBIR1* and *TaSERKs*. The corresponding proteins were successfully detected in inputs, and only *TaSERK2* and *TaSERK5* were co-immunoprecipitated by *TaBIR1* (Figure 7B), further confirming the interaction between *TaBIR1* with *TaSERK2* and *TaSERK5*.

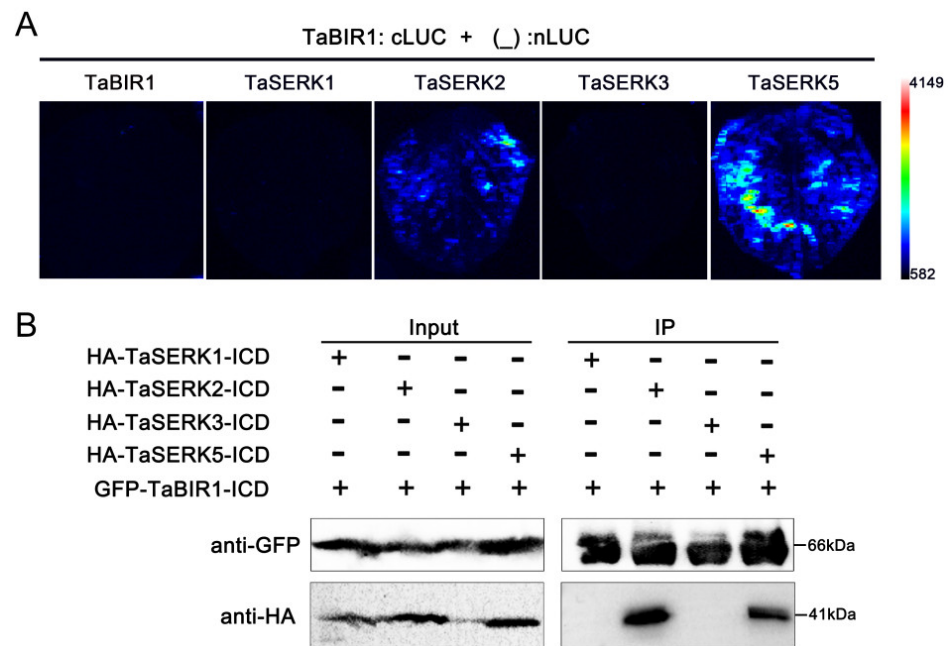


**Figure 7.** TaBIR1 associates with TaSERK2 and TaSERK5. (A) Interaction between TaBIR1 and TaSERK2, TaSERK5 confirmed by split-luciferase assay. *TaBIR1*:cLUC and indicated proteins with C-terminal nLUC were co-expressed in *N. benthamiana* by agroinfiltration. Images of chemiluminescence were recorded by applying 0.5 mM luciferin at 48 h after infiltration. (B) Interaction between TaBIR1 and TaSERK2, TaSERK5 verified by Co-IP assay. Intracellular domains (ICD) of *TaSERKs* were individually co-expressed with GFP tagged *TaBIR1* in *N. benthamiana*. Total proteins were extracted and immunoprecipitated by anti-GFP Agarose beads. The total proteins and immunoprecipitated proteins were detected using anti-GFP and anti-HA antibody.

Since *TaBIR1* mediated immune responses in *N. benthamiana* depending on *NbBAK1* and that TaBIR1 associates with TaSERK2/TaSERK5, we tested if *TaSERK2* and *TaSERK5* could restore *TaBIR1* triggered immunity in *NbBAK1* silencing plants. Comparing to the seldom callose deposits in *NbBAK1* silencing plants expressing *TaBIR1* alone, the co-expression of *TaBIR1* and *TaSERK2* or *TaSERK5* in *NbBAK1* silenced leaves led to much more abundant callose deposition, but not when co-expressed with *TaSERK1* or *TaSERK3* (Figure 8). Additionally, co-expression of *TaBIR1* and *TaSERK2* or *TaSERK5* result in significant ROS burst and cell death in *NbBAK1* silenced leaves (Figure S4). Together, these results indicated that wheat *TaSERK2* and *TaSERK5* could compensate the role of *NbBAK1*.

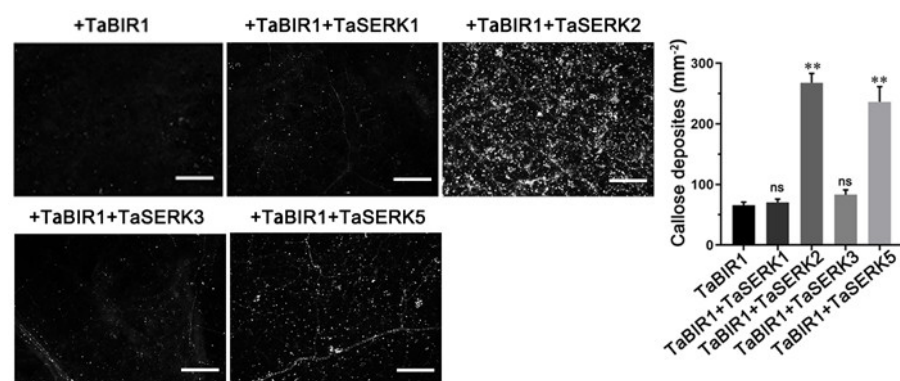


**Figure 8.** Heterologous expression of *TaSERK2* and *TaSERK5* restored the immunity triggered by *TaBIR1* in *NbBAK1*-silenced *N. benthamiana* leaves. Two weeks after inoculation of TRV2:*NbBAK1*, *TaSERKs* and *TaBIR1* were co-expressed in the corresponding plant leaves. Forty-eight hours later, the

leaves were collected for aniline blue staining. The number of callose deposits per mm<sup>2</sup> in *NbBAK1*-silenced leaves co-expressing *TaSERKs* and *TaBIR1* was quantified. Values represent the means  $\pm$  standard errors from three independent biological samples (n = 30). Differences were assessed compared with that in leaves expressing *TaBIR1* alone using Student's *t*-tests (\*\* *p* < 0.01, ns, no significance). Bars, 200  $\mu$ m.

### 3. Discussion

Planting resistant wheat cultivars is the most effective way to control wheat stripe rust. Nonetheless, *P. striiformis* continuously adapts to overcome host immunity, resulting in the ineffectiveness of disease-resistant varieties. Identifying novel resistant resources of durable resistance is of great importance for sustainable control of stripe rust. Extracellular receptor-mediated resistance tends to be broad-spectrum and durable due to the recognition of conserved microbial molecules, which provides an important genetic resource for the creation of broad-spectrum disease resistance materials.

Transfer of EF-Tu receptor EFR, which is unique to cruciferous plants, into tomato, tobacco, rice, wheat and other plants, can improve the broad-spectrum resistance of genetically improved crops to bacterial diseases [39]. The rice bacterial blight resistance gene *XA21*, which recognizes the highly conserved AX21 in bacteria, confers broad-spectrum resistance to *Xanthomonas oryzae* [17,18]. The rice transcription factor gene, *OsAP2/ERF152*, is transferred, which results in the induction of callose deposition, cell death, and enhanced resistance against infection by *Xanthomonas oryzae* pv. *oryzae* [40]. Additionally, its expression in Arabidopsis transgenics activated the MPK3/6 and exhibited broad-spectrum resistance to *Pseudomonas syringae* pv. *tomato* DC3000 and *Rhizoctonia solani* AG1-IA [41]. The introduction of the *LecRK-V* gene from *Haynaldia villosa* into wheat variety YANG-MAI158 mediates broad-spectrum resistance to powdery mildew [42]. Exploration of the regulation mechanism of PRR receptor and signal transduction may provide an important theoretical basis for the creation of broad-spectrum disease resistance crop materials. However, because of the large genome of common hexaploid wheat, the identification and functional study of wheat extracellular receptor genes are very limited. Here, we identified an important plasma-membrane receptor *TaBIR1* that positively modulates plant immunity and contributes wheat resistance to stripe rust. Knockdown of *TaBIR1* compromised wheat immunity against *Pst* with impaired ROS burst, callose accumulation and cell death occurrence. Heterologous overexpression of *TaBIR1* in *N. benthamiana* activated basal immunity with HR-like cell death, suggesting its potential use in improving wheat resistance. Deciphering the mechanism of *TaBIR1* mediated immunity is critical for its proper use in resistance engineering.

*BAK1*-interacting receptor-like kinase (*BIR1*) is a negative regulator of *BAK1* and *SO-BIR1*-mediated immune response. In Arabidopsis, loss function of *BIR1* leads to constitutive activation of cell death, enhanced accumulation of SA and H<sub>2</sub>O<sub>2</sub>, and induction of *PR* genes dependent on *BAK1*, *EDS1*, *PAD4*, and *SOBIR1* in the absence of pathogen infection [29]. The inactivation of *BIR1* triggers resistance to TRV [43]. Similarly, transient silencing *GmBIR1*, a *BIR1* homologue gene in soybean, also resulted in activated defense response and enhanced resistance to *Pseudomonas syringae* pv. *glycinea* (*Psg*) and Soybean mosaic virus (SMV) [44]. It seems that the function of *BIR1* homologues as a negative regulator of immunity is conserved among different plant species. However, our study revealed the positive role of *TaBIR1* in inducing cell death, callose deposition and ROS production in *N. benthamiana*, the knockdown of which in wheat attenuates resistance to stripe rust with decreased ROS and callose accumulation. *BIR1* homologues between dicot Arabidopsis and monocot wheat plants seems to play divergent roles in plant immunity regulation.

In fact, exploration on the relevance of *BIR1* regulation in infected plants revealed that *BIR1* overexpression causes morphological defects and limited TRV accumulation in *N. benthamiana* cells. Additionally, transgenic Arabidopsis with inducible *BIR1* overexpression stimulated an autoimmune response as observed in *bir1-1* without pathogen infection [43]. Both low and high expression of *BIR1* were concomitant to defense responses,

assuming that *BIR1*-associated phenotypes are dose-dependent, and there is a threshold for the proper function of *BIR1*. It is not clear whether there is such a threshold for *TaBIR1*. Probably, the observed triggered defense is due to exceeds of the threshold, leading to the mis-regulation of plant immunity. Knockout mutants of *TaBIR1* are needed to demonstrate its role in cell death control and defense response regulation under pathogen free and pathogen infection environment in the future study.

*BIR1* belongs to BIR family, including four members (*BIR1*-*BIR4*). Evidence showed that BIRs have evolved partially redundant but also distinct functions. *BIR2* knock mutant also exhibits enhanced PAMP responses, but does not have the dwarf morphology, like *bir1-1*. Over-expression of *BIR1* does not affect flg22-induced immune responses, while the over-expression of *BIR2* attenuates PAMP-triggered responses [27,28]. *BIR2* constitutively interacts with BAK1 in the absence of ligands, which upon ligand activation is released from the complex, and thus, BAK1 can associate with the ligand-bound receptor complex partners. In contrast to the other BIRs, *BIR3* associates not only with BAK1 but also with all functional SERKs, thereby exhibiting a general molecular mechanism compared to the relatively specialized function of *BIR2*. The overexpression of *BIR3* leads to a strong dwarf phenotype and significant blocking of BR responses, indicating its strong impact on both BR- and microbe-associated molecular pattern (MAMP)-induced responses, but its weak cell death control. It seems that although the BIR family proteins share similar sequence and domain structure, duplication events within the BIR subfamily of LRR-RLKs have evolved new molecular functions and mechanisms [45–47]. *BIR1* is an active kinase [29]. Multiple alignments showed that *TaBIR1* exhibits mutations in conserved kinase motifs comparing to *BIR1*, which likely influence its kinase activity. Moreover, the cell death and defense response in *bir1-1* is mediated by both BAK1 and SOBIR1, but *TaBIR1* triggered cell death in BAK1-dependent manner but not SOBIR1, suggesting their different downstream signaling pathway. Further studies on the kinase activity of *TaBIR1* and its functional pathway will be necessary to deeply illustrate its distinct functional manner.

BAK1 is a central regulator of innate immunity in multiple receptor complexes and interacts with *BIR1* family member [29,42,48]. *TaBIR1* affects plant cell death and defense response required BAK1. Interestingly, we demonstrated that *TaBIR1* associates with wheat BAK1 homologues TaSERK2 and TaSERK5. Moreover, TaSERK2 and TaSERK5 could compensate the repaired defense response caused by *BAK1* silencing. These results indicate the general regulatory role of BAK1 homologues in immune signaling by membrane-associated receptors among plant species as co-receptors, and a functional link of *TaBIR1* with co-receptors. They may exist in the uncovered PRR complex since all of them are regulatory kinases that not response for ligand binding. BAK1, on one hand, could serve as a positive regulator in basal resistance against the bacterial pathogen *Pseudomonas syringae* pv. *tomato* DC3000 and the oomycete pathogen *Hyaloperonospora arabidopsidis*, and on the other hand, is involved in negative regulation of R protein mediated immunity. Knocking out both *BAK1* and its close homolog *BKK1* lead to strong autoimmune phenotypes [49]. In this way, the specifically regulatory roles of *TaBIR1* are possibly determined by the involved receptor complex under different signaling pathway. The role of BAK1-resistance pathway needs further investigation to elucidate its contribution to *TaBIR1* mediated stripe rust resistance. Additionally, the additional components in *TaBIR1*-TaSERK2/TaSERK5 module, especially the PRR with its potential ligand needs to be further investigated.

In summary, our work demonstrates a wheat extracellular receptor gene *TaBIR1*, which contributes to wheat resistance against *Pst*. We demonstrate that the membrane-localized receptor *TaBIR1* functionally associated with TaSERK2/TaSERK5 to activate immune responses. The new insights gained from the characterization of this receptor-like kinase will help to engineer PRR-based broad-spectrum resistant crop varieties.

## 4. Materials and Methods

### 4.1. Plant Growth, Conditions and Pathogen Infection

Plant materials include wheat cultivar Suwon11 (Su11) and *N. benthamiana* were used in this study. For wheat seedlings, plants were grown in a controlled growth chamber (16 h:8 h, light:dark, 16 °C:10 °C). Fresh urediospores of *Pst* race CYR23 (avirulent on Su11), CYR31 (virulent on Su11), were collected and inoculated according to the procedures described previously [50]. As for *N. benthamiana*, seedlings were grown in the growth chamber at 23 °C (16 h:8 h, light:dark). *Agrobacterium tumefaciens* strain GV3101 was used in infiltration assay for transient expression in *N. benthamiana*.

### 4.2. Total RNA Extraction and qRT-PCR Analysis

For RNA isolation, samples of wheat and *N. benthamiana* leaves were collected and total RNA was isolated using Trizol reagent (Invitrogen, Carlsbad, CA, USA) according to the manufacturer's instructions. Two microgram of total RNA was used for reverse transcription using Revert Aid First Strand cDNA Synthesis Kit (Ferments, Waltham, MA, USA). All qRT-PCR reactions were conducted on a CFX Connect Real-Time System (Bio-Rad, Hercules, CA, USA). Gene relative expression was analyzed using the comparative  $2^{-\Delta\Delta CT}$  method with three biological replications [51]. Data significance was evaluated by Student's *t*-test. All primers used in qRT-PCR were listed in Table S1.

### 4.3. Sequence Analysis, Alignment and Polymorphism Analysis

Prediction of conserved domains and motifs were performed by PROSITE Scan (<http://prosite.expasy.org/scanprosite/>, accessed on 8 May 2020) and SMART (<http://smart.embl.de/>, accessed on 8 May 2020). DNAMAN 6.0 was used to achieve the multi-sequence alignments. Phylogenetic tree was created by the MEGA software (Version 7.0, Kumar S, Philadelphia, PA, USA).

### 4.4. Subcellular Localization

For subcellular localization in wheat mesophyll protoplasts, seedlings were kept dark for one day just before use to block the chloroplast auto-fluorescence. Wheat mesophyll protoplasts were prepared using seven-day-old leaves with digestion in the enzyme buffer. Constructions of *TaBIR1-GFP* and *GFP* were transformed to protoplasts using polyethylene glycol (PEG) calcium transfection according to the method described by Yoo et al. [52]. Green fluorescence signals were monitored 18 h after transformation.

For subcellular localization in *N. benthamiana* cells, *Agrobacterium* GV3101 strain carrying *TaBIR1-GFP* and *GFP* reconstructed plasmids were cultured in LB (Luria-Bertani) medium containing 50  $\mu\text{g mL}^{-1}$  rifampicin and 50  $\mu\text{g mL}^{-1}$  kanamycin at 28 °C. Cells were collected after shaking and resuspended in acetosyringone (AS) buffer (10 mM  $\text{MgCl}_2$ , 10 mM MES, pH 5.6, and 120  $\mu\text{M}$  acetosyringone) at a final  $\text{OD}_{600}$  of 0.6 and then infiltrated into *N. benthamiana* leaves. GFP fluorescence was observed 48 h later. Plasmolysis was performed by submerging leaves into 0.8 M mannitol for 10 min.

All photos were taken by FV1000 MPE confocal laser microscope (Olympus, Tokyo, Japan) with assays repeated at least three times.

### 4.5. BSMV-Mediated Gene Silencing

For Barley Stripe Mosaic Virus (BSMV) assay in wheat, two silencing fragments (VIGS-1, VIGS-2) were designed and combined to specifically knock down *TaBIR1* transcript. Each fragment was evaluated by BLASTn against wheat genome to ensure specific silencing. Both fragments were cloned and inserted into BSMV: $\gamma$  vector as previously described [53]. Plasmids were linearized and transcribed using the T7 in vitro transcription kit (Promega) following the manufacturer's instructions. The transcripts of BSMV:*TaBIR1* (containing VIGS-1, VIGS-2) mixed with BSMV: $\alpha$ , BSMV: $\beta$ , and FES buffer were inoculated on the second leaves of two-leaf stage wheat seedlings. TaPDS encoding *T. aestivum* phytoene desaturase was used as silencing index. A fragment of *GFP* was used as negative control.

After virus inoculation, infected plants were maintained in a controlled growth chamber at 25 °C. Twelve days later, the fully expanded fourth leaves were further inoculated with fresh *Pst* CYR23 urediospores and maintained at 16 °C. The *Pst* inoculated leaves were collected at 0, 24, 48 hpi for silencing efficiency and histochemical assays. Samples at 240 h for fungal biomass was analyzed as described [54].

#### 4.6. TRV-Mediated Silencing in *N. benthamiana*

For silencing assay in *N. benthamiana*, *A. tumefaciens* GV3101 cells carrying pTRV2-*NbSOBIR1*, pTRV2-*NbBAK1*, pTRV2-*NbPDS*, pTRV2-*GFP* were mixed individually with *A. tumefaciens* harboring pTRV1 in 1:1 ratio to a final OD<sub>600</sub> of 0.2 and then infiltrated into cotyledons of four-leaf-stage seedlings. The pTRV2-*NbPDS* was used as an index for effective silencing and pTRV2-*GFP* was used as negative control. Two weeks later, when pTRV2-*NbPDS* silencing plants showed photo-bleaching, GV3101 carrying recombinant HA tagged *TaBIR1* were infiltrated into the corresponding leaves of pTRV2-*NbSOBIR1*, pTRV2-*NbBAK1*, pTRV2-*NbPDS*, and pTRV2-*GFP* silencing plants. Samples were collected at 48 h for subsequent immune analysis.

#### 4.7. Transient Over-Expression in *N. benthamiana*

For *A. tumefaciens*-mediated transient expression, GV3101 carrying the recombinant constructs of *GFP* fused full length *TaBIR1* and *GFP* control were cultured and infiltrated into 4-week-old *N. benthamiana* leaves individually using 1-mL needleless syringe. At 48 h later, *GFP* fluorescence was checked for successful expression and samples were collected for immune responses detection.

#### 4.8. Histochemical Observations and Immune Responses Detection

In the in situ detection of H<sub>2</sub>O<sub>2</sub> in wheat challenged by *Pst*, leaves were incubated in the 1 mg mL<sup>-1</sup> 3,3-diaminobenzidine (DAB) solution for 6 h under a strong light. After the DAB solution was absorbed, samples were destained (absolute ethyl alcohol: acetic acid, 1:1, *v/v*) until the chlorophyll was completely removed. Then, leaf segments were immersed in chloral hydrate overnight for more transparent. Samples were preserved in 50% glycerol and the DAB polymerized reddish-brown spots produced at infection site was observed in bright channel under Olympus BX-53 microscope (Olympus Corp., Tokyo, Japan). For observation of callose deposits, destained wheat leaves were stained with 0.05% aniline blue in 0.067 M K<sub>2</sub>HPO<sub>4</sub> (pH 9.0) overnight [55] and observed under UV channel of Olympus BX-53 microscope. Number of callose deposits per mm<sup>2</sup> were calculated by ImageJ software (1.52a version). For the observation of hyphae, the infected tissues were cleared with ethanol as described above and boiled in 2 mL of 1 M KOH at 100 °C for 10 min. Leaves were then washed three times with 50 mM Tris-HCl (pH 7.4) for 10 min, followed by wheat germ agglutinin (WGA) staining that conjugated to Alexa-488 (Invitrogen) and observed by an Olympus BX-53 microscope. For each sample, thirty infection sites that a substomatal vesicle formed were examined and calculated using DP-BSW software (Olympus Corp., Tokyo, Japan) with Student's *t*-test for the statistical analyses.

In *N. benthamiana*, for H<sub>2</sub>O<sub>2</sub> observation, whole leaves were immersed into 1 mg mL<sup>-1</sup> DAB solution with gently shaking for 6 h under light and then boiled in absolute ethyl alcohol for destaining. Observation of callose deposits was performed following the same method in wheat. As for cell death assay, samples were collected and stained with Trypan Blue solution (10 mL of lactic acid, 10 mL of glycerol, 10 g of phenol, 10 mg of trypan blue, dissolved in 10 mL of distilled water) and boiled for 5 min, then decolorized in chloral hydrate until tissue completely transparent [56]. Leaves were observed under UV channel of Olympus BX-53 microscope.

For the measurement of total reactive oxygen species (ROS) content in wheat and *N. benthamiana* leaves, samples were ground in liquid nitrogen, and extracted in PBS solution (1 g mL<sup>-1</sup>) with 12,000 rpm centrifugation at 4 °C for 10 min. Supernatants were

used to determine ROS concentration according to the instructions of Plant ROS ELISA kit (BioTSZ, E60016).

#### 4.9. Protein Interaction

The luciferase complementation assay was performed in *N. benthamiana* leaves as previously described [57]. Briefly, *A. tumefaciens* GV3101 harboring the nLUC and cLUC constructs (all respective RLKs fused at the N-terminal to keep LUC fragments in cytoplasmic) were co-infiltrated into *N. benthamiana* leaves. Forty-eight hours later, leaves were taken and treated with 0.5 mM luciferin. The LUC activity was measured by the Lumazine Pylon 2048B (Princeton, NJ, USA).

For Co-IP assay, intracellular domain (ICD) of all *TaSERKs* in fusion with HA and FLAG tag (HA at C-terminal, FLAG at N-terminal) were amplified and inserted into the PICH86988 vector. *A. tumefaciens* GV3101 carrying individual *TaSERKs*-ICD-PICH vectors together with *TaBIR1*-ICD-pBinGFP were co-expressed in *N. benthamiana*. The infiltrated leaves were collected at 48 h later, ground in liquid nitrogen and extracted in a buffer (50 mM Tris-HCl, pH 7.5, 150 mM NaCl, 10% glycerol, 10 mM DTT, 1 mM NaF, 1 mM Na<sub>2</sub>MoO<sub>4</sub>·2H<sub>2</sub>O, 1 mM PMSE, 1% [v/v] P9599 Protease Inhibitor Cocktail, 1% [v/v] IGEPAL CA-630 [Sigma-Aldrich] (St. Louis, MO, USA)). After 12,000 rpm centrifugation at 4 °C for 10 min, each supernatant was incubated with 25 µL GFP-Trap agarose beads (Chromotek, gta-20) for 2 h followed by four times washing. The supernatant and total protein were immunoblotted by anti-HA antibody (Abbkine, A02045) and anti-GFP antibody (Abbkine, A02020). All primers used are listed in Table S1.

## 5. Conclusions

The current research characterized a wheat LRR-RLK *TaBIR1* that functions as a positive regulator of wheat resistance against the biotrophic fungus *P. striiformis*. As a membrane-localized RLK, *TaBIR1* requires the co-receptor NbBAK1 to modulate plant basal immunity in *N. benthamiana*. Moreover, wheat BAK1 homologues *TaSERK2* and *TaSERK5* could restore the function of NbBAK1 in *TaBIR1* triggered immunity, indicating a *TaBIR1*-*TaSERK2*/*TaSERK5* immune signaling pathway, which possibly contribute to wheat resistance to *Pst*. Given the short LRRs of *TaBIR1*, we assume that it might participate in a receptor complex to modulate immune outputs for establishing plant resistance. Our findings will provide a further understanding on the regulation of immune receptor complex in hexaploid wheat, and a potentially utilized genetic resource in crop improvement.

**Supplementary Materials:** The following supporting information can be downloaded at: <https://www.mdpi.com/article/10.3390/ijms24076438/s1>.

**Author Contributions:** C.T., Z.K. and X.W. designed the research program; Y.S., F.L., H.G. and Z.W. conducted the experiments; C.T. and Y.S. wrote the manuscript; Z.K. and J.W. revised the manuscript. All authors have read and agreed to the published version of the manuscript.

**Funding:** This work was supported by the National Natural Science Foundation of China (Grants 32293243), National Key R&D Program of China (2021YFD1401000), and the 111 Project from the Ministry of Education of China (BP0719026).

**Institutional Review Board Statement:** Not applicable.

**Informed Consent Statement:** Not applicable.

**Data Availability Statement:** The data used in this research is publicly available. The gene sequences can be found at <https://www.ncbi.nlm.nih.gov/>, accessed on 2 July 2021 (*TaSERK1*, Accession no. AK333001; *TaSERK2*, Accession no. AK333677.1; *TaSERK3*, Accession no. BT009223; *TaSERK5*, Accession no. BT009426). The data (results) presented in this research are available in the Supplementary Materials.

**Acknowledgments:** The authors are very grateful to Guorong Wei from Northwest A&F University for providing the *Pst* races CYR23/CYR31, and Hua Zhao and Fengping Yuan from Northwest A&F University for their technical support in confocal microscopy observation.

**Conflicts of Interest:** The authors declare no conflict of interest.

## References

1. Boller, T.; Felix, G. A renaissance of elicitors: Perception of microbe-associated molecular patterns and danger signals by pattern-recognition receptors. *Annu. Rev. Plant Biol.* **2009**, *60*, 379–407. [[CrossRef](#)] [[PubMed](#)]
2. Schwessinger, B.; Ronald, P.C. Plant innate immunity: Perception of conserved microbial signatures. *Annu. Rev. Plant Biol.* **2012**, *63*, 451–482. [[CrossRef](#)] [[PubMed](#)]
3. Jones, J.D.; Dangl, J.L. The plant immune system. *Nature* **2006**, *444*, 323–329. [[CrossRef](#)] [[PubMed](#)]
4. Dodds, P.N.; Rathjen, J.P. Plant immunity: Towards an integrated view of plant-pathogen interactions. *Nat. Rev. Genet.* **2010**, *11*, 539–548. [[CrossRef](#)]
5. Monaghan, J.; Zipfel, C. Plant pattern recognition receptor complexes at the plasma membrane. *Curr. Opin. Plant Biol.* **2012**, *15*, 349–357. [[CrossRef](#)]
6. Ngou, B.; Ahn, H.K.; Ding, P.; Jones, J.D. Mutual potentiation of plant immunity by cell-surface and intracellular receptors. *Nature* **2021**, *592*, 110–115. [[CrossRef](#)]
7. Yuan, M.; Jiang, Z.; Bi, G.; Nomura, K.; Liu, M.; Wang, Y.; Cai, B.; Zhou, J.; He, S.; Xin, X. Pattern-recognition receptors are required for NLR-mediated plant immunity. *Nature* **2021**, *592*, 105–109. [[CrossRef](#)]
8. Zhou, J.; Zhang, Y. Plant immunity: Danger perception and signaling. *Cell* **2020**, *181*, 978–989. [[CrossRef](#)]
9. Shiu, S.H.; Karlowski, W.M.; Pan, R.; Tzeng, Y.H.; Mayer, K.F.; Li, W.H. Comparative analysis of the receptor-like kinase family in Arabidopsis and rice. *Plant Cell* **2004**, *16*, 1220–1234. [[CrossRef](#)]
10. Gomez-Gomez, L.; Boller, T. FLS2: An LRR receptor-like kinase involved in the perception of the bacterial elicitor flagellin in Arabidopsis. *Mol. Cell* **2000**, *5*, 1003–1011. [[CrossRef](#)]
11. Chinchilla, D.; Zipfel, C.; Robatzek, S.; Kemmerling, B.; Nürnberger, T.; Jones, J.D.; Felix, G.; Boller, T. A flagellin-induced complex of the receptor FLS2 and BAK1 initiates plant defence. *Nature* **2007**, *448*, 497–500. [[CrossRef](#)]
12. Zipfel, C.; Kunze, G.; Chinchilla, D.; Caniard, A.; Jones, J.D.; Boller, T.; Felix, G. Perception of the bacterial PAMP EF-Tu by the receptor EFR restricts *Agrobacterium*-mediated transformation. *Cell* **2006**, *125*, 749–760. [[CrossRef](#)]
13. Gao, M.; Liu, J.; Bi, D.; Zhang, Z.; Cheng, F.; Chen, S.; Zhang, Y. MEKK1, MKK1/MKK2 and MPK4 function together in a mitogen-activated protein kinase cascade to regulate innate immunity in plants. *Cell Res.* **2008**, *18*, 1190–1198. [[CrossRef](#)]
14. Lu, D.; Wu, S.; Gao, X.; Zhang, Y.; Shan, L.; He, P. A receptor-like cytoplasmic kinase, BIK1, associates with a flagellin receptor complex to initiate plant innate immunity. *Proc. Natl. Acad. Sci. USA* **2010**, *107*, 496–501. [[CrossRef](#)]
15. Sun, T.; Nitta, Y.; Zhang, Q.; Wu, D.; Tian, H.; Lee, J.S.; Zhang, Y. Antagonistic interactions between two MAP kinase cascades in plant development and immune signaling. *EMBO Rep.* **2018**, *19*, e45324. [[CrossRef](#)]
16. Li, L.; Li, M.; Yu, L.; Zhou, Z.; Liang, X.; Liu, Z.; Cai, G.; Gao, L.; Zhang, X.; Wang, Y.; et al. The FLS2-associated kinase BIK1 directly phosphorylates the NADPH oxidase RbohD to control plant immunity. *Cell Host Microbe* **2014**, *15*, 329–338. [[CrossRef](#)]
17. Song, W.; Wang, G.; Chen, L.; Kim, H.; Pi, L.; Holsten, T.; Gardner, J.; Wang, B.; Zhai, W.; Zhu, L.; et al. A receptor kinase-like protein encoded by the rice disease resistance gene, *Xa21*. *Science* **1995**, *270*, 1804–1806. [[CrossRef](#)]
18. Pruitt, R.N.; Schwessinger, B.; Joe, A.; Thomas, N.; Liu, F.; Albert, M.; Robinson, M.R.; Chan, L.J.; Luu, D.D.; Chen, H.; et al. The rice immune receptor XA21 recognizes a tyrosine-sulfated protein from a Gram-negative bacterium. *Sci. Adv.* **2015**, *1*, e1500245. [[CrossRef](#)]
19. Liu, T.; Liu, Z.; Song, C.; Hu, Y.; Han, Z.; She, J.; Fan, F.; Wang, J.; Jin, C.; Chang, J.; et al. Chitin-induced dimerization activates a plant immune receptor. *Science* **2012**, *336*, 1160–1164. [[CrossRef](#)]
20. Cao, Y.; Liang, Y.; Tanaka, K.; Nguyen, C.T.; Jedrzejczak, R.P.; Joachimiak, A.; Stacey, G. The kinase LYK5 is a major chitin receptor in Arabidopsis and forms a chitin-induced complex with related kinase CERK1. *eLife* **2014**, *3*, e03766. [[CrossRef](#)]
21. Kaku, H.; Nishizawa, Y.; Ishii-Minami, N.; Akimoto-Tomiyama, C.; Dohmae, N.; Takio, K.; Minami, E.; Shibuya, N. Plant cells recognize chitin fragments for defence signalling through a plasma membrane receptor. *Proc. Natl. Acad. Sci. USA* **2006**, *103*, 11086–11091. [[CrossRef](#)] [[PubMed](#)]
22. Shimizu, T.; Nakano, T.; Takamizawa, D.; Desaki, Y.; Ishii-Minami, N.; Nishizawa, Y.; Minami, E.; Okada, K.; Yamane, H.; Kaku, H.; et al. Two LysM receptor molecules, CEBiP and OsCERK1, cooperatively regulate chitin elicitor signalling in rice. *Plant J.* **2010**, *64*, 204–214. [[CrossRef](#)] [[PubMed](#)]
23. Wang, C.; Wang, G.; Zhang, C.; Zhu, P.; Dai, H.; Yu, N.; He, Z.; Xu, L.; Wang, E. OsCERK1-mediated chitin perception and immune signaling requires receptor-like cytoplasmic kinase 185 to activate an MAPK cascade in rice. *Mol. Plant* **2017**, *10*, 619–633. [[CrossRef](#)] [[PubMed](#)]
24. Ma, X.; Xu, G.; He, P.; Shan, L. SERKING coreceptors for receptors. *Trends Plant Sci.* **2016**, *21*, 1017–1033. [[CrossRef](#)]
25. Hohmann, U.; Santiago, J.; Nicolet, J.; Olsson, V.; Spiga, F.M.; Hothorn, L.A.; Butenko, M.A.; Hothorn, M. Mechanistic basis for the activation of plant membrane receptor kinases by SERK-family coreceptors. *Proc. Natl. Acad. Sci. USA* **2018**, *115*, 3488–3493. [[CrossRef](#)]
26. Schulze, B.; Mentzel, T.; Jehle, A.K.; Mueller, K.; Beeler, S.; Boller, T.; Felix, G.; Chinchilla, D. Rapid heteromerization and phosphorylation of ligand-activated plant transmembrane receptors and their associated kinase BAK1. *J. Biol. Chem.* **2010**, *285*, 9444–9451. [[CrossRef](#)]
27. Halter, T.; Imkamp, J.; Mazzotta, S.; Wierzba, M.; Postel, S.; Bucherl, C.; Kiefer, C.; Stahl, M.; Chinchilla, D.; Wang, X.; et al. The leucine-rich repeat receptor kinase BIR2 is a negative regulator of BAK1 in plant immunity. *Curr. Biol.* **2014**, *24*, 134–143. [[CrossRef](#)]

28. Liu, Y.; Huang, X.; Li, M.; He, P.; Zhang, Y. Loss-of-function of Arabidopsis receptor-like kinase BIR1 activates cell death and defense responses mediated by BAK1 and SOBIR1. *New Phytol.* **2016**, *212*, 637–645. [[CrossRef](#)]
29. Gao, M.; Wang, X.; Wang, D.; Xu, F.; Ding, X.; Zhang, Z.; Bi, D.; Cheng, Y.; Chen, S.; Li, X.; et al. Regulation of cell death and innate immunity by two receptor-like kinases in Arabidopsis. *Cell Host Microbe* **2009**, *6*, 34–44. [[CrossRef](#)]
30. Roux, M.; Schwessinger, B.; Albrecht, C.; Chinchilla, D.; Jones, A.; Holton, N.; Malinovsky, F.G.; Tör, M.; de Vries, S.; Zipfel, C. The Arabidopsis leucine-rich repeat receptor-like kinases BAK1/SERK3 and BKK1/SERK4 are required for innate immunity to hemibiotrophic and biotrophic pathogens. *Plant Cell* **2011**, *23*, 2440–2455. [[CrossRef](#)]
31. Chen, X.; Zuo, S.; Schwessinger, B.; Chern, M.; Canlas, P.E.; Ruan, D.; Zhou, X.; Wang, J.; Daudi, A.; Petzold, C.J.; et al. An XA21-associated kinase (OsSERK2) regulates immunity mediated by the XA21 and XA3 immune receptors. *Mol. Plant* **2014**, *7*, 874–892. [[CrossRef](#)]
32. Fradin, E.F.; Zhang, Z.; Ayala, C.J.; Castroverde, D.M.; Nazar, R.N.; Robb, J.; Liu, C.M.; Thomma, H.J. Genetic dissection of *Verticillium* wilt resistance mediated by tomato *Ve1*. *Plant Physiol.* **2009**, *150*, 320–332. [[CrossRef](#)]
33. Goodin, M.M.; Zaitlin, D.; Naidu, R.A.; Lommel, S.A. *Nicotiana benthamiana*: Its history and future as a model for plant-pathogen interactions. *Mol. Plant Microbe Interact.* **2015**, *1*, 28–39. [[CrossRef](#)]
34. Wang, X.; Tang, C.; Zhang, G.; Li, Y.; Wang, C.; Liu, B.; Qu, Z.; Zhao, J.; Han, Q.; Huang, L.; et al. cDNA-AFLP analysis reveals differential gene expression in compatible reaction of wheat challenged with *Puccinia striiformis* f. sp. tritici. *BMC Genom.* **2009**, *10*, 289–300. [[CrossRef](#)]
35. Chinchilla, D.; Shan, L.; He, P.; de Vries, S.; Kemmerling, B. One for all: The receptor-associated kinase BAK1. *Trends Plant Sci.* **2009**, *14*, 535–541. [[CrossRef](#)]
36. Liebrand, T.W.; van den Burg, H.A.; Joosten, M.H. Two for all: Receptor associated kinases SOBIR1 and BAK1. *Trends Plant Sci.* **2014**, *19*, 123–132. [[CrossRef](#)]
37. Singla, B.; Khurana, J.P.; Khurana, P. Characterization of three somatic embryogenesis receptor kinase genes from wheat, *Triticum aestivum*. *Plant Cell Rep.* **2008**, *27*, 833–843. [[CrossRef](#)]
38. Singh, A.; Khurana, P. Ectopic expression of *Triticum aestivum* SERK genes (TaSERKs) control plant growth and development in Arabidopsis. *Sci. Rep.* **2017**, *7*, 12368–12381. [[CrossRef](#)]
39. Lacombe, S.; Rougon-Cardoso, A.; Sherwood, E.; Peeters, N.; Dahlbeck, D.; van Esse, H.P.; Smoker, M.; Rallapalli, G.; Thomma, B.P.; Staskawicz, B.; et al. Interfamily transfer of a plant pattern-recognition receptor confers broad-spectrum bacterial resistance. *Nat. Biotechnol.* **2010**, *28*, 365–369. [[CrossRef](#)]
40. Jha, G.; Patel, H.K.; Dasgupta, M.; Palaparthi, R.; Sonti, R.V. Transcriptional profiling of rice leaves undergoing a hypersensitive response like reaction induced by *Xanthomonas oryzae* pv. *oryzae* cellulase. *Rice* **2010**, *3*, 1–21. [[CrossRef](#)]
41. Pillai, S.E.; Kumar, C.; Dasgupta, M.; Kumar, B.K.; Vungarala, S.; Patel, H.K.; Sonti, R.V. Ectopic expression of a Cell-Wall-Degrading Enzyme-Induced *OsAP2/ERF152* leads to resistance against bacterial and fungal infection in Arabidopsis. *Phytopathology* **2020**, *110*, 726–733. [[CrossRef](#)] [[PubMed](#)]
42. Wang, Z.; Cheng, J.; Fan, A.; Zhao, J.; Yu, Z.; Li, Y.; Zhang, H.; Xiao, J.; Muhammad, F.; Wang, H.; et al. *LecRK-V*, an L-type lectin receptor kinase in *Haynaldia villosa*, plays positive role in resistance to wheat powdery mildew. *Plant Biotechnol. J.* **2018**, *16*, 50–62. [[CrossRef](#)] [[PubMed](#)]
43. Guzmán-Benito, I.; Donaire, L.; Amorim-Silva, V.; Vallarino, J.G.; Esteban, A.; Wierzbicki, A.T.; Ruiz-Ferrer, V.; Llave, C. The immune repressor BIR1 contributes to antiviral defense and undergoes transcriptional and post-transcriptional regulation during viral infections. *New Phytol.* **2019**, *224*, 421–438. [[CrossRef](#)] [[PubMed](#)]
44. Liu, D.; Lan, H.; Masoud, H.; Ye, M.; Dai, X.; Zhong, C.; Tian, S.; Liu, J. Silencing *GmBIR1* in Soybean results in activated defense responses. *Int. J. Mol. Sci.* **2022**, *23*, 7450–7462. [[CrossRef](#)]
45. Russinova, E.; Borst, J.W.; Kwaaitaal, M.; Cano-Delgado, A.; Yin, Y.; Chory, J.; de Vries, S.C. Heterodimerization and endocytosis of Arabidopsis brassinosteroid receptors BRI1 and AtSERK3 (BAK1). *Plant Cell* **2004**, *16*, 3216–3229. [[CrossRef](#)]
46. Imkampe, J.; Halter, T.; Huang, S.; Schulze, S.; Mazzotta, S.; Schmidt, N.; Manstretta, R.; Postel, S.; Wierzbza, M.; Yang, Y.; et al. The Arabidopsis leucine-rich repeat receptor kinase BIR3 negatively regulates BAK1 receptor complex formation and stabilizes BAK1. *Plant Cell* **2017**, *29*, 2285–2303. [[CrossRef](#)]
47. Jaillais, Y.; Belkhadir, Y.; Balsemão-Pires, E.; Dangl, J.L.; Chory, J. Extracellular leucine-rich repeats as a platform for receptor/coreceptor complex formation. *Proc. Natl. Acad. Sci. USA* **2011**, *108*, 8503–8507. [[CrossRef](#)]
48. Heese, A.; Hann, D.R.; Gimenez-Ibanez, S.; Jones, A.M.; He, K.; Li, J.; Schroeder, J.I.; Peck, S.C.; Rathjen, J.P. The receptor-like kinase SERK3/BAK1 is a central regulator of innate immunity in plants. *Proc. Natl. Acad. Sci. USA* **2007**, *104*, 12217–12222. [[CrossRef](#)]
49. Kemmerling, B.; Schwedt, A.; Rodriguez, P.; Mazzotta, S.; Frank, M.; Qamar, S.A.; Mengiste, T.; Betsuyaku, S.; Parker, J.E.; Mussig, C.; et al. The BRI1-associated kinase 1, BAK1, has a brassinolide-independent role in plant cell death control. *Curr. Biol.* **2007**, *17*, 1116–1122. [[CrossRef](#)]
50. Kang, Z.; Huang, L.; Buchenauer, H. Ultrastructural changes and localization of lignin and callose in compatible and incompatible interactions between wheat and *Puccinia striiformis*. *J. Plant Dis. Protect.* **2002**, *109*, 25–37.
51. Livak, K.J.; Schmittgen, T.D. Analysis of relative gene expression data using real-time quantitative PCR and the  $2^{-\Delta\Delta CT}$  Method. *Methods* **2001**, *25*, 402–408. [[CrossRef](#)]
52. Yoo, S.D.; Cho, Y.H.; Sheen, J. Arabidopsis mesophyll protoplasts: A versatile cell system for transient gene expression analysis. *Nat. Protoc.* **2007**, *2*, 1565–1572. [[CrossRef](#)]

53. Holzberg, S.; Brosio, P.; Gross, C.; Pogue, G.P. Barley stripe mosaic virus-induced gene silencing in a monocot plant. *Plant J.* **2002**, *30*, 315–327. [[CrossRef](#)]
54. Liu, J.; Han, L.; Huai, B.; Zheng, P.; Chang, Q.; Guan, T.; Li, D.; Huang, L.; Kang, Z. Down-regulation of a wheat alkaline/neutral invertase correlates with reduced host susceptibility to wheat stripe rust caused by *Puccinia striiformis*. *J. Exp. Bot.* **2015**, *66*, 7325–7338. [[CrossRef](#)]
55. Hood, M.E.; Shew, H.D. Applications of KOH-aniline blue fluorescence in the study of plant-fungal interactions. *Phytopathology* **1996**, *86*, 704–708. [[CrossRef](#)]
56. Wang, C.; Huang, L.; Buchenauer, H.; Han, Q.; Zhang, H.; Kang, Z. Histochemical studies on the accumulation of reactive oxygen species ( $O_2^-$  and  $H_2O_2$ ) in the incompatible and compatible interaction of wheat–*Puccinia striiformis* f. sp. tritici. *Physiol. Mol. Plant P.* **2007**, *71*, 230–239. [[CrossRef](#)]
57. Chen, H.; Zou, Y.; Shang, Y.; Lin, H.; Wang, Y.; Cai, R.; Tang, X.; Zhou, J. Firefly luciferase complementation imaging assay for protein-protein interactions in plants. *Plant Physiol.* **2008**, *146*, 368–376. [[CrossRef](#)]

**Disclaimer/Publisher’s Note:** The statements, opinions and data contained in all publications are solely those of the individual author(s) and contributor(s) and not of MDPI and/or the editor(s). MDPI and/or the editor(s) disclaim responsibility for any injury to people or property resulting from any ideas, methods, instructions or products referred to in the content.